THE ASTROPHYSICAL JOURNAL, 359:4–14, 1990 August 10

CLASSIFICATION OF GALAXIES ON CCD FRAMES

SIDNEY VAN DEN BERGH AND MICHAEL J. PIERCE
Dominion Astrophysical Observatory, National Research Council of Canada
AND
R. BRENT TULLY
Institute for Astronomy, University of Hawaii
Received 1989 November 14; accepted 1990 February 9

ABSTRACT

New morphological classifications are given for 231 galaxies in or near the Virgo and Ursa Major clusters. It is found that classification of galaxies on CCD frames is more accurate than are classifications based on inspection of photographic plates. Our classifications show that the Virgo Cluster contains a class of spiral galaxies with large central "bulges," that exhibit strong or moderately strong star formation near their centers. The outer regions of these objects frequently exhibit a smooth "anemic" appearance. Very few galaxies of this type were found in the Ursa Major Cluster. It is tentatively suggested that *the early-type spiral galaxies with active star formation in their central regions, which are observed in the Virgo Cluster, might represent a mild form of the Butcher-Oemler effect that still survives at zero redshift.*

For 29 Virgo galaxies with Tully-Fisher distances $D < 20$ Mpc the mean distance modulus, as derived from luminosity classifications, is $(m-M) = 30.93 \pm 0.13$ (15.3 Mpc). This may be compared with $(m-M) = 31.57 \pm 0.17$ (20.8 Mpc) from luminosity classifications of eight galaxies which have Tully-Fisher (TF) distances $D > 20$ Mpc. The *difference* between the distance moduli of TF background and cluster members is $\Delta(m-M) = 0.66 \pm 0.21$. This result strongly supports the conclusion that the large dispersion in the TF relation for galaxies in the Virgo direction is largely due to contamination of the cluster core sample by background galaxies. Adding the 0.31 mag systematic uncertainty in the luminosity of the calibrating galaxies in quadrature yields a distance modulus $(m-M) = 30.93 \pm 0.34$ ($15.3^{+2.6}_{-2.2}$ Mpc) for the core of the Virgo Cluster. This value is, within the quoted errors, consistent with recent distance determinations based on planetary nebulae and the Tully-Fisher technique.

The dustiness of Virgo and Ursa Major cluster galaxies is found to drop dramatically below $B_T \simeq 13$ ($M_B \simeq -18$).

Subject headings: galaxies: clustering — galaxies: distances — galaxies: interstellar matter — galaxies: structure

I. INTRODUCTION

The DDO system of galaxy classification (van den Bergh 1960*a*, *b*, *c*, 1966) was based on visual inspection of galaxy images on the blue prints of the Palomar Sky Survey. This data base had the advantage that it provided images of uniform quality for a very large number of galaxies. Disadvantages of using the paper prints of the Palomar Sky Survey for classification purposes are that (1) the dynamic range is small, so that the nuclear regions of bright galaxies tend to be burned out, (2) the original singlet corrector plate of the Palomar 1.2 m Schmidt telescope produced rather large stellar images with FWHM of $\sim 2''$, and (3) it was not possible to distinguish unambiguously between E and S0 galaxies.

In the present paper we use CCD images of galaxies, obtained with the 2.2 m and 0.6 m telescopes of the University of Hawaii, for classifications of galaxies. The classification system adopted in the present paper, which will subsequently be referred to as the DAO system, contains elements of both the original DDO system and its revised version (van den Bergh 1976*a*). The digital data used in our new investigation have the advantage of a large dynamic range, which can be fully explored with an interactive image display system. This makes it easy to study details of both the inner and outer structure of galaxies. A disadvantage of the present data base is, however, that it is more difficult to use the contrast between sky and galaxy images as a classification parameter because some exposures were obtained in moonlight (for less than 10% of the data). Nevertheless, it has been our experience that the advantages of galaxy classification on digital images greatly outweigh their disadvantages.

II. CLASSIFICATIONS

The images used to classify the galaxies discussed in this paper were obtained as part of an ongoing photometric survey of nearby galaxies (e.g., Pierce 1988; Pierce and Tully 1988). The data constitute *B*-band CCD images of a complete sample of spiral and irregular galaxies in the Virgo and Ursa Major clusters. The Ursa Major sample includes galaxies within 7°.5 of $\alpha = 11^h54^m$, $\delta = +49°30'$ (epoch 1950) with 700 km s^{-1} < $V_0 < 1210$ km s^{-1} (where V_0 is the velocity corrected for a solar motion of 300 km s^{-1} toward $l = 90°$, $b = 0°$), and brighter than the limit of the CfA 14.5 mag survey (Huchra *et al.* 1983), corresponding to a tilt-corrected limit of $B_T = 13.3$. The Virgo sample (cf. Binggeli, Sandage, and Tammann 1985) was above all acquired for the purpose of employing the Tully-Fisher method to study infall into the cluster. The sample completeness characteristics are therefore tainted by the needs of that program. The completeness criteria employed were that all galaxies (i) are located within an area bounded by $12^h5^m < \alpha < 13^h0^m$ and $+2° < \delta < +19°$; (ii) have Hubble types later or equal to Sa; (iii) have inclinations greater than 30° (based on Sky Survey axial ratios); (iv) have Zwicky magnitudes less than 15.2 (whence $B_T^i \lesssim 14.0$). Furthermore, (v) galaxies that were manifestly pathological in morphology were excluded, as were (vi) galaxies in which the H I emission was confused with that of neighboring galaxies or with Galactic H I emission. Note that the sample includes systems drawn from both the traditional 6° radius Virgo Cluster centered on M87 and the adjacent "southern extension" and "Virgo W" (de Vaucouleurs 1961) clouds. *All* galaxies within the 6° cluster brighter than $B_T = 12.0$ have been observed, as have many fainter elliptical and S0 galaxies with measured velocity dispersions, which are useful for the three-parameter Faber-Jackson distance estimator method, and a random assortment of fainter disk systems, reaching as faint as $B_T = 15.9$.

The data were acquired in one of two observing configurations: (1) Galaxies with $D_{25} \gtrsim 5'.0$ were imaged with a TI 500 × 500 thinned, backside illuminated CCD behind an f/3 focal reducer on the University of Hawaii 0.6 m telescope, yielding a scale of $1''.6$ pixel^{-1} and a field of view of 13′ square. (2) Galaxies with $D_{25} \lesssim 5'.0$ were imaged with either a TI 500 × 500 CCD or an NSF/TI 800 × 800 CCD, behind the f/2 focal reducer on the University of Hawaii 2.2 m telescope. These configurations resulted in a scale of $0''.67$ pixel^{-1}, and fields of view of 5′ and 7′, respectively. Integration times were 10 minutes for the 0.6 m observations and 5 minutes for the 2.2 m observations. In cases of nuclear saturation, short exposures were also obtained. Very low surface brightness levels were reached (typically $\mu_B \sim 27$ mag arcsec^{-2}). Anything visible on the Palomar Sky Survey could be seen in a 20 s integration with the 0.6 m telescope. Individual galaxy classifications that were made during the course of the present program are listed in Table 1. Most classifications of galaxies with $B < 12$ were performed on images obtained with the 0.6 m telescope, whereas all fainter galaxies were classified on frames taken with the 2.2 m telescope. Agreement between independent classifications of a few galaxies with both 0.6 m and 2.2 m images was excellent.

Column (1) of Table 1 lists the NGC or UGC number, or the VCC designation (Binggeli, Sandage, and Tammann 1985), for each of the program galaxies. Column (2) gives the cluster assignment. In the subsequent discussion "Vir" galaxies will be referred to as members of the Virgo Cluster proper. Column (3) gives the new DAO type of each galaxy, and column (4) the Hubble type taken from Sandage and Tammann (1981) or, failing that, from Binggeli, Sandage, and Tammann (1985). The apparent total blue magnitude of each galaxy is listed in column (5). These values were taken from Pierce (1988) or, failing that, from Sandage and Tammann (1981) or from Binggeli, Sandage, and Tammann (1985). Note that these magnitudes are *not* corrected for internal absorption. Column (6) gives radial velocities V_0 of galaxies (corrected for a solar motion of 300 km s^{-1} directed toward $l = 90°$, $b = 0$). These velocities were taken from a variety of sources, with preference given to values derived from 21 cm observations. In column (7), 88 and 24 refer to the 2.2 m and 0.6 m telescopes, respectively. An asterisk in the last column of the table indicates that an object is a "Virgo-type" galaxy. (This classification type is explained in §§ III and IV*g*.) The classifications listed in Table 1 define the DAO system. For galaxies that are too faint to exhibit spiral structure the presence of a nucleus, or of a nuclear bulge, was used to distinguish between the S and Ir classification types. In the present classification system we have only assigned early-type objects that contain a clear disklike substructure to class S0. For example, we classify NGC 4370 (which has a strong equatorial dust lane) as Epec, whereas Binggeli, Sandage, and Tammann (1985) assign it to type $S0_3$ because of its dust lane. In most cases it was only possible to distinguish between classification types E and S0 in edge-on, or nearly edge-on, galaxies. We note in passing that dust lanes and dust clouds at the distance of the Virgo Cluster are much easier to see on 2.2 m images than they are on 0.6 m images. On the prints of the Palomar Sky Survey it is often difficult to distinguish elliptical and blue compact galaxies (BCGs). This problem does not arise in the case of digital CCD images.

III. SOME PECULIARITIES OF VIRGO CLUSTER GALAXIES

The Palomar Sky Survey provided the first large homogeneous survey of galaxies. Inspection of the Sky Survey images of spiral galaxies (van den Bergh 1960*b*) showed subtle differences between field galaxies and galaxies in rich clusters, such as the Virgo and Coma clusters. The most striking of these differences was a tendency for many Virgo galaxies of type Sb to have fuzzy outer spiral structure. In the DDO classification system such objects were denoted as Sbn or, in extreme cases, as Snn. It was initially assumed that this morphological peculiarity was due to past galaxy interactions. Later work (van den Bergh 1976*a*, *b*) showed that the anemic appearance of the outer structure of spirals in rich clusters, such as Virgo and Coma, was more likely due to gas deficiency produced by ram-pressure stripping (Gunn and Gott 1972). It was subsequently emphasized by Zasov (1975) that such ram-pressure stripping would be most severe in the outer regions of spiral galaxies. Ram-pressure stripping is also likely to be the cause of the small size of the hydrogen disks of spirals near the center of the Virgo Cluster (van Gorkom and Kotanyi 1985). The prediction that the spirals in rich clusters should be gas-poor has been strongly confirmed by all subsequent 21 cm line studies (e.g., Giovanelli and Haynes 1985; Haynes and Giovanelli 1986). There is also evidence, at the 3 σ level (van den Bergh 1984), that Virgo spirals are dust-poor compared with similar objects in the field. More recently this conclusion has received considerable observational support from an analysis of *IRAS* observations by Doyon and Joseph (1989).

Kenney and Young (1989) have shown that Virgo spirals are *less* deficient in CO than they are in neutral hydrogen. They find that those luminous Sc galaxies, which are deficient in H I by a factor of 10, have star formation rates (as judged by Hα emission) that are only a factor of 2 or 3 lower than normal. From a comparison of CO and 21 cm line emission Kenney and Young find that most neutral hydrogen has been stripped from the outer regions of Virgo spirals, whereas the dense CO-emitting clouds in the central regions of these objects have been retained. This suggests that the rate of star formation might only be low in the outer regions of anemic galaxies. Because the inner regions of many spirals are saturated, it is not, in general, possible to check this hypothesis on the prints of the Palomar Sky Survey. The present digital data do allow one to search for star formation in the dense inner regions of both anemic and normal spirals. Such a search shows that the Virgo Cluster contains a class of galaxies with fuzzy or anemic outer spiral structure and active star formation in their inner regions. Examples of objects of this type are shown in Figures 1 and 2. Some galaxies of this type exhibit a superficial resemblance to objects of Hubble type Sa. However, digital data show that their central "bulges" are *not* primarily composed of

TABLE 1

CLASSIFICATIONS OF GALAXIES IN AND NEAR THE VIRGO AND UMA CLUSTERS

Name (1)	Cl. (2)	DAO type (3)	Hubble type (4)	B_T (5)	V_o (6)	Tel. (7)	Remark (8)
NGC 3718	UMa	St/Merger	Sa pec?	11.6	1068	24	...
NGC 3726	UMa	S(B)c I-II	Sc I-II	10.9	914	24	4
NGC 3729	UMa	S(B?)c pec III-IV:	SB pec	12.4	1117	88	5,6,*
NGC 3769	UMa	S(B)bt	SBc II	12.7	773	24	...
NGC 3782	UMa	SIV	SBm IV	13.2	793	88	...
NGC 3870	UMa	Amorphous?	...	13.7	2491	88	...
NGC 3877	UMa	SbIII	Sc II.2	11.8	954	24	...
NGC 3893	UMa	Sbc II-III: (t?)	Sc I.2	11.2	1043	24	4
NGC 3898	(UMa)	Sb II	Sa I.2	11.7	1272	88	15
NGC 3906	UMa	SB IV	...	...	...	88	...
NGC 3917	UMa	SIII-IV	Sc III	12.6	1056	24	...
NGC 3938	UMa	Sbc II	Sc I	11.0	852	24	...
NGC 3949	UMa	BCG	Sc III	11.6	868	24	7
NGC 3953	UMa	S(B)bc I-II	SBbc I-II	11.0	1139	88,24	...
NGC 3972	UMa	SIII-IV	...	13.1	947	24	...
NGC 3977	UMa	Sa/SO	...	...	600	24	...
NGC 3985	UMa	Sc III-IV	S	13.0	820	88	5
NGC 3990	UMa	SO	...	13.6	1238	88	...
NGC 3998	UMa	E	SO	11.5	968	88	10
NGC 4010	UMa	Sc/Ir	...	13.3	...	88	1
NGC 4013	UMa	Sa	Sbc:	12.3	883	24	1
NGC 4026	UMa	SO	SO	11.7	958	24	1
NGC 4051	UMa	Sbc II	Sbc II	11.0	763	24	...
NGC 4085	UMa	Sc III-IV	Sc III:	13.2	794	88	2,7
NGC 4088	UMa	Sc pec III	Sc II-III/SBc	11.3	844	24	...
NGC 4100	UMa	Sc pec II	Sc I-II	12.0	1153	88	7
NGC 4102	UMa	S(B?)c III:	Sb II	12.1	953	88	5
NGC 4111	UMa	SO	SO	11.5	842	24	...
NGC 4116	Vir SE?	SBIV	SBc III	12.4	1177	88	...
NGC 4123	Vir SE?	SBb II	SBbc	11.8	1207	88	...
NGC 4124	Vir	SO	SO	12.2	1551	24	...
NGC 4142	UMa	Sc IV	...	...	1257	88	...
NGC 4152	Vir	Sbc II	Sc I.4	12.5	2086	88	...
NGC 4157	UMa	S	Sbc	12.2	854	24	1
NGC 4178	Vir	S(B)b III	SBc II	12.1	284	24	...
NGC 4183	UMa	Sb III:	Scd	13.0	987	24	1
NGC 4189	Vir	Sc pec	SBc II.2	12.6	2031	88	4
NGC 4192	Vir	Sb II	Sb II:	11.0	-220	24	...
NGC 4193	Vir M?	Sbc II	Sc II	13.2	2381	88	7
NGC 4197	Vir W	Sb	Scd	13.5	1948	88	*
NGC 4206	Vir	SIII-IV	Sc	12.9	616	24	2
NGC 4207	Vir	S	Scd	13.5	507	88	1,*?
NGC 4212	Vir	Sc/BCG	Sc II-III	11.9	-163	24	7,*?
NGC 4216	Vir	Sb II-III	Sb	10.8	490	24	2,4
NGC 4217	UMa	Sb III:	Sb:	12.0	1098	88,24	1

Name (1)	Cl. (2)	DAO type (3)	Hubble type (4)	B_T (5)	V_o (6)	Tel. (7)	Remark (8)
NGC 4220	UMa	A(?)II-III:	Sa	12.4	1052	88	...
NGC 4222	Vir	Sd	Scd	13.9	143	88	1
NGC 4233	Vir W?	E/SO	SBO	13.0	2117	88	...
NGC 4237	Vir	Sc II-III	Sc II.8	12.5	871	88	...
NGC 4254	Vir	Sc I	Sc I.3	10.4	2323	24	...
NGC 4262	Vir	E pec	SBO	12.6	1290	88	8
NGC 4267	Vir	E	SBO	12.0	1177	24	...
NGC 4273	Vir W	S(B)bc III-IV:	SBc II	12.4	2234	88	4,*
NGC 4277?	Vir	A(B)	SBa	14.5	...	88	...
NGC 4289	Vir W	Ab	Sbc	14.3	2424	88	1
NGC 4298	Vir	SIV	Sc III	12.1	1044	24	...
NGC 4302	Vir	Scd	Sc	12.6	1044	24	1
NGC 4305	Vir	Ab I	Sa	13.3	1846	88	9
NGC 4306	Vir	E	d:SBO	13.8	...	88	4
NGC 4307	Vir	Sab II-III	Sb?	12.8	994	88	*?
NGC 4312	Vir	Sa III-IV	Sab	12.6	84	88	2,*
NGC 4313	Vir	SIV:	Sab	12.7	1357	88	3,*
NGC 4316	Vir	S	Sbc	13.7	1149	88	1,*?
NGC 4321	Vir	Sc I	Sc I	10.0	1522	24	...
NGC 4330	Vir	Sd:	Sd	13.1	1477	88	1
NGC 4340	Vir	SBO/SBa	SBO	12.2	790	24	...
NGC 4342	Vir	E	E7	13.2	609	88	...
NGC 4343	Vir	Sab III	Sb	13.1	908	88	2,7,*?
NGC 4346	UMa	SO	...	12.2	922	88	10
NGC 4350	Vir	SO	SO	11.9	1120	24	...
NGC 4351	Vir	Sc III-IV	Sc II.3	13.2	2214	88	*
NGC 4353	Vir	BCG	Sc II-III	13.1	1073	88	7,*?
NGC 4365	Vir	E	E3	10.4	1091	24	10
NGC 4369	...	SO	Sc III-IV	12.3	680	24	14
NGC 4370	Vir	E pec	SO	13.7	...	88	2,3
NGC 4371	Vir	S(B)O	SBO	11.8	897	24	...
NGC 4374	Vir	E	E1	10.0	854	24	...
NGC 4376	Vir SE	BCG	Scd III	13.9	1026	88	7?,*
NGC 4380	Vir	Sb I-II	Sab	12.5	872	88	...
NGC 4382	Vir	SO	SO pec	9.8	717	24	11
NGC 4383	Vir	Amorphous	SO:	12.8	1545	88	...
NGC 4389	UMa	Sc pec	SB pec	12.6	...	88	...
NGC 4390	Vir	Sb III	Sbc II	13.3	1009	88	...
NGC 4396	Vir	SIV	Sc II	13.0	-194	88	...
NGC 4402	Vir	SIV	Sc	12.6	156	88	1,3
NGC 4406	Vir	E:	SO/E3	9.9	-419	24	...
NGC 4411	Vir	S(B) IV	SBc II	13.6	1186	88	...
NGC 4412	Vir SE	Sbc II:	SBbc II	13.1	2185	88	...
NGC 4416	Vir	S(B)cd III-IV	SBc II.2	12.9	1294	88	4
NGC 4417	Vir	SO	SO	12.2	733	24	1

TABLE 1—*Continued*

Name (1)	Cl. (2)	DAO type (3)	Hubble type (4)	B_T (5)	V_o (6)	Tel. (7)	Remark (8)
NGC 4419	Vir	Sa pec	SBab:	12.2	-342	24	1
NGC 4420	Vir SE	SIII-IV	Sc III	12.7	1557	88	*?
NGC 4421	Vir	SBO	SBO	12.4	1625	88	10
NGC 4423	Vir W	Ir/S	Sd	14.3	984	88	1
NGC 4424	Vir	S/A	S(a?) pec	12.4	366	88	*?
NGC 4425	Vir	SO pec	SBO pec/Sa pec	12.9	1804	88	10
NGC 4429	Vir	Aa	SO/Sa pec	10.9	1028	24	...
NGC 4430	Vir W?	S(B) III: (t?)	SBc II	12.5	1344	88	4,*?
NGC 4435	Vir	E	SBO	11.6	792	24	...
NGC 4436	Vir	SO	dE6/dSO	14.0	...	88	...
NGC 4438	Vir	St!	Sb (tides)	11.1	182	24	...
NGC 4440	Vir	ABb II	SBa	12.7	...	88	11
NGC 4442	Vir	S(B)O	SBO	11.5	489	24	8
NGC 4450	Vir	Ab II:	Sab pec	11.0	1899	24	...
NGC 4451	Vir	A/S	Sc III	13.4	600	88	...
NGC 4458	Vir	E	E1	13.1	308	24	...
NGC 4459	Vir	E	SO	11.3	1039	24	...
NGC 4461	Vir	SO	Sa	12.2	1811	24	...
NGC 4466	Vir	S	Sc:	14.6	...	88	*
NGC 4470	Vir	Sc IV	Sc III pec	13.0	2241	88	7?
NGC 4472	Vir	E	E1/SO	9.3	847	24	...
NGC 4473	Vir	E	E5	11.1	2205	24	...
NGC 4477	Vir	SBO	SBO/SBa	11.5	1190	24	...
NGC 4479	Vir	SBO/SBa	SBO	13.5	749	24	...
NGC 4480	Vir SE	Sbc II	Sb II	13.1	2326	88	...
NGC 4483	Vir	SO/SBO	SBO	13.3	903	88	...
NGC 4486	Vir	E	EO	9.7	1181	24	10
NGC 4496	Vir SE	SBc III	SBc III-IV	11.7	1619	88	...
NGC 4498	Vir	S(B)c III	SBc II	12.9	1448	88	...
NGC 4501	Vir	Sbc I	Sbc II	10.4	2217	24	...
NGC 4502	Vir	SIV	Sm III	14.6	1335	88	*?
NGC 4503	Vir	SO	Sa	12.2	1136	24	...
NGC 4519	Vir	Sc II-III	SBc II.2	12.6	2241	88	...
NGC 4522	Vir	A(c?)	Sc/Sb:	13.1	354	88	*
NGC 4526	Vir	S(B?)O	SO	10.6	...	24	8
NGC 4527	Vir SE	Sb pec	Sb II	11.3	1614	88	3,*
NGC 4531	Vir	SIII-IV	Sa pec	12.6	122	88	7,*
NGC 4532	Vir	BCG	Sm III-IV	12.3	1909	88	...
NGC 4535	Vir	S(B)b I-II	SBc I.3	10.7	1873	24	...
NGC 4536	Vir SE	S(B)c I-II	Sc I	11.0	1748	88	...
NGC 4539	Vir	SO	...	...	1243	88	2,11
NGC 4540	Vir	SIV	Scd III-IV	12.9	1224	88	7,*
NGC 4544	Vir SE	Sa	Sc	13.9	1033	88	1,*?
NGC 4548	Vir	SBb/ABb II	SBb I-II	11.0	406	24	...
NGC 4552	Vir	EO	SO	11.2	165	88	10
NGC 4564	Vir	SO/E	E6	12.2	942	88	10
NGC 4567	Vir	Sc pec	Sc II-III	12.1	2139	24	11
NGC 4568	Vir	Sc pec	Sc II-III	11.7	2168	24	11
NGC 4569	Vir	Ab II:	Sab I-II	10.4	-383	24	3,*
NGC 4570	Vir	SO	SO/E7	11.9	1634	24	1
NGC 4571	Vir	Sbc II	Sc II-III	12.1	282	88	...
NGC 4579	Vir	A(B)b II	Sab II	10.5	1729	24	...
NGC 4584	Vir	A/Sa	Sa pec	13.7	...	88	6
NGC 4586	Vir SE	A/Sa	Sa	12.5	722	88	...
NGC 4591	Vir SE?	Sa	Sb	13.7	2317	88	*?
NGC 4595	Vir	Sc III-IV	Sc II.8	13.2	601	88	...
NGC 4596	Vir	SBO/SBa	SBa	11.3	1939	24	...
NGC 4606	Vir	SIV	Sa pec	12.7	1610	88	3
NGC 4607	Vir	S/Ir	Scd	13.8	2178	88	1,3
NGC 4608	Vir	SBO/SBa	SBO/a	12.0	1789	24	...
NGC 4621	Vir	E	E5	10.7	340	24	...
NGC 4623	Vir	E/SO	E7	13.4	1873	88	...
NGC 4630	Vir SE	Sa?	S	13.0	587	88	*
NGC 4633	Vir	SIV	Scd	13.8	228	88	...
NGC 4634	Vir	S/Ir	Sc	13.2	56	88	1,3,11
NGC 4638	Vir	E/SO	SO	12.3	1006	24	...
NGC 4639	Vir	S(B)b II	SBb II	12.4	917	88	...
NGC 4647	Vir	Sc pec	Sc III	12.0	1285	24	7
NGC 4649	Vir	E	SO	9.7	1127	24	10?
NGC 4651	Vir	SbII/AbII	Sc I-II	11.5	748	24	*
NGC 4654	Vir	Sb III:	SBc II	11.1	978	24	*?
NGC 4660	Vir	E	E5	11.4	943	88	...
NGC 4666	Vir SE	Sb III-IV	Sbc II.3	11.6	1395	88	7
NGC 4689	Vir	Sb/Ab	Sb II.3	11.8	1715	88	*?
NGC 4698	Vir	Sa	Sa	11.6	905	24	...
NGC 4701	Vir SE	Sab III	Sbc II	12.8	624	88	*
NGC 4713	Vir SE?	S(B)c III?	SBc II-III	12.2	560	88	4
NGC 4746	Vir	S	...	...	1714	88	1,3
NGC 4753	Vir SE?	SO pec	SO pec	10.8	1102	88	11
NGC 4754	Vir	S(B)O	SBO	11.5	1393	24	...
NGC 4758	Vir?	S/Ir	...	...	1196	88	1,4
NGC 4762	Vir	SO pec	SO	11.0	874	24	1,12
NGC 4765	Vir SE	BCG?	Sd III:	13.3	687	88	7
NGC 4771	Vir SE	Sa III	Sc II-III:	12.7	...	88	*?
NGC 4772	Vir SE?	Sa III	Sa:	12.4	982	88	...
NGC 4779	Vir?	SBb II	...	...	...	88	...
NGC 4808	Vir SE	SIV	Sc III	12.6	668	88	...
NGC 4845	Vir SE	Ab III	Sa	12.2	1124	88	3
NGC 4866	Vir?	Ab II-III:	Sa	11.8	1912	88	...
UGC 6399	UMa	SIV	...	14.4	873	88	...

TABLE 1—*Continued*

Name (1)	Cl. (2)	DAO type (3)	Hubble type (4)	B_T (5)	V_o (6)	Tel. (7)	Remark (8)
UGC 6446	UMa	Sc III	...	13.7	725	88	7
UGC 6606	UMa	pec	...	...	...	24	...
UGC 6628	UMa	Sc III-IV	...	13.3	901	88	7
UGC 6667	UMa	Scd	...	14.4	1051	88	1
UGC 6781	UMa	pec	...	...	...	24	...
UGC 6816	UMa	S(B)IV	...	14.4	998	88	...
UGC 6917	UMa	SBc III	...	13.3	996	88	...
UGC 6923	UMa	SIV pec	...	14.0	1172	88	...
UGC 6930	UMa	S(B)c III	...	12.8	851	88	...
UGC 6962	UMa	S(B)IV	...	13.0	827	88	...
UGC 6973	UMa	S pec	...	13.1	756	88	2,*
UGC 6983	UMa	SBbc III	...	13.3	1166	88	...
UGC 7181	Vir	SBb III:	Sc:	14.6	180	88	...
UGC 7209	Vir M	S(B)b II	SBb I-II	13.5	2144	88	11
UGC 7216	Vir	SIV	Sc pec	14.0	...	88	...
UGC 7218	UMa	Ir IV-V	...	15.0	882	88	...
UGC 7249	Vir	Ir IV-V	...	15.7	541	88	...
UGC 7279	Vir M?	S/Ir	Sd	15.0	1883	88	1
UGC 7326	Vir	S/Ir IV	Sd	14.6	-245	88	1
UGC 7333	Vir	A(B)b III:	SBbc I-II	13.8	...	88	...
UGC 7352	Vir W?	SIV-V	SBcd III	14.5	2363	88	...
UGC 7423	Vir	SIV-V	Sd/Sm IV	15.0	...	88	...
UGC 7470	Vir	SIV	Sc III-IV	13.8	-517	88	*
UGC 7479	Vir	S/Ir IV-V	...	...	...	88	...
UGC 7513	Vir	Sc	Sc	13.7	898	88	1
UGC 7518	Vir	Sb	Sc	14.1	...	88	1
UGC 7522	Vir SE	Ac/Sc	Sc	14.6	1304	88	...
UGC 7546	Vir	Sbc III-IV	Sc II	13.1	1170	88	...
UGC 7547	Vir	V	...	15.4	1016	88	...
UGC 7563	Vir	SIV-V	Scd III	14.2	2271	88	...
UGC 7567	Vir	S/Ir IV-V	Sdm III	14.8	...	88	...
UGC 7590	Vir	SIV	Sbc I.8	14.6	...	88	...
UGC 7602	Vir	SIV	Sc/Sa	13.3	1615	88	7,*
UGC 7612	Vir SE	S(B)IV-V	SBcd II	14.1	1452	88	...
UGC 7621	Vir	S/Ir IV	Sc II	13.7	440	88	4,*
UGC 7676	Vir	SIII-IV	SBc II-III	14.0	...	88	5,*
UGC 7695	Vir	SIII-IV pec	Sc II.2	13.3	-241	88	13
UGC 7733	Vir	Ir IV-V	...	...	347	88	...
UGC 7736	Vir	Ir IV	SBm pec	14.0	496	88	*
UGC 7784	Vir	Ir IV	Sm III	13.9	1055	88	*?
UGC 7790	Vir?	Ir IV	SBm III	14.1	...	88	*
UGC 7822	Vir	S/Ir IV	...	14.6	1995	88	...
UGC 7920	Vir	S? IV-V	Amorphous	13.7	781	88	2,*
UGC 7932	Vir	S/Ir IV	SBc II	13.9	901	88	...
UGC 7943	Vir SE?	SIII-IV	...	...	743	88	...
UGC 7982	Vir SE	S	...	...	1063	88	1
VCC 888	Vir	Ir(B)/S(B) IV-V	Im III	15.9	...	88	4
VCC 1356	Vir	BCG	Sm III/BCD	14.9	...	88	*
VCC 1431	Vir	E	dEO	14.5	...	24	...
VCC 1654	Vir	Ir IV-V	Im III	15.0	...	88	...
VCC 1725	Vir	Ir	Sm III/BCD	14.5	...	88	...

REMARKS.—(1) Edge-on. (2) Almost edge-on. (3) Very dusty. (4) Asymmetric. (5) Single arm. (6) Merger? (7) Has nucleus. (8) Isophote twist. (9) Spiral structure possibly induced by interaction with NGC 306. (10) Has globular clusters. (11) Possible tidal interactions. (12) Very thin disk, swept Sc? (13) Thin filament of dust and stars crosses main body of galaxy. (14) This galaxy appears to have been misclassified in Sandage and Tammann 1981. (15) Possibly background galaxy (Tully 1988).

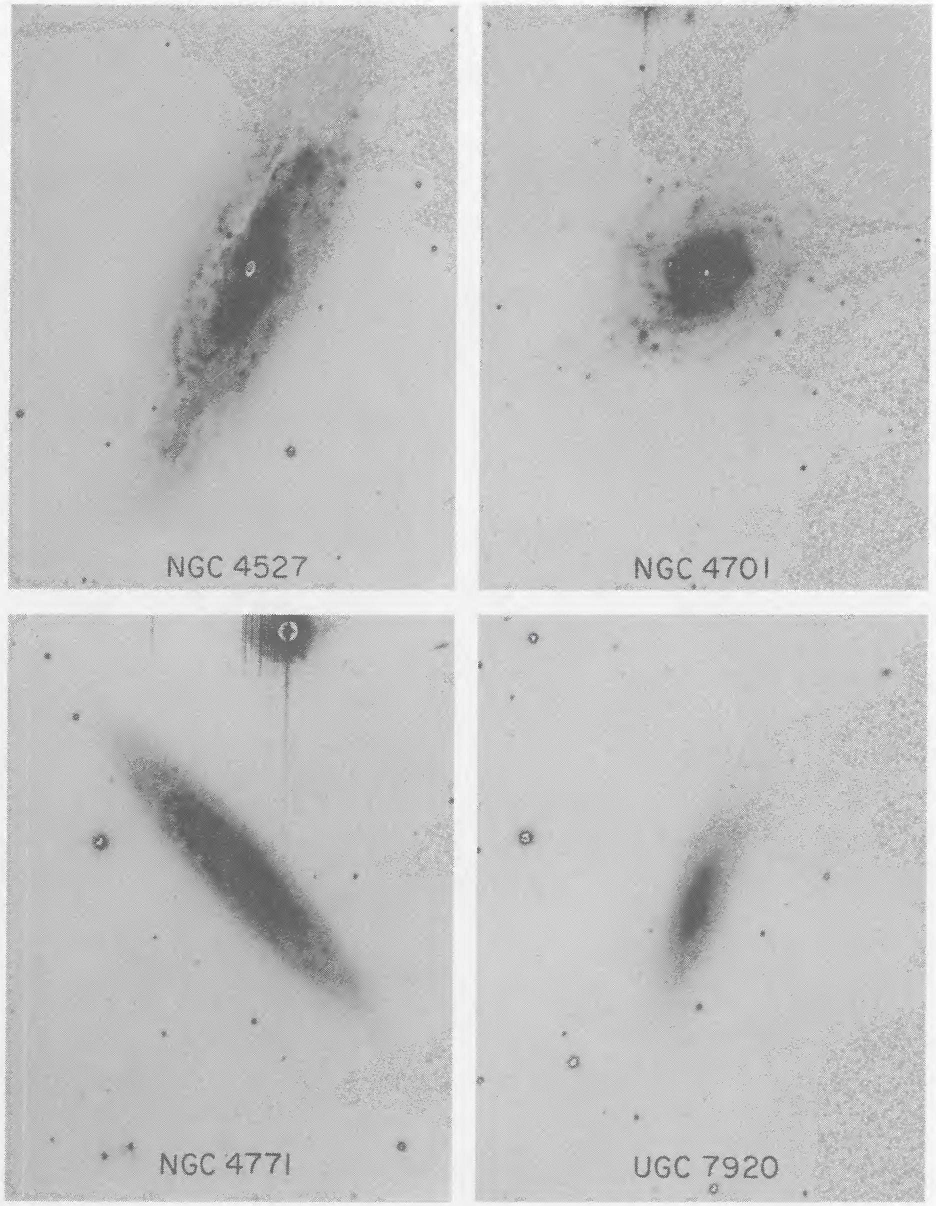

FIG. 1

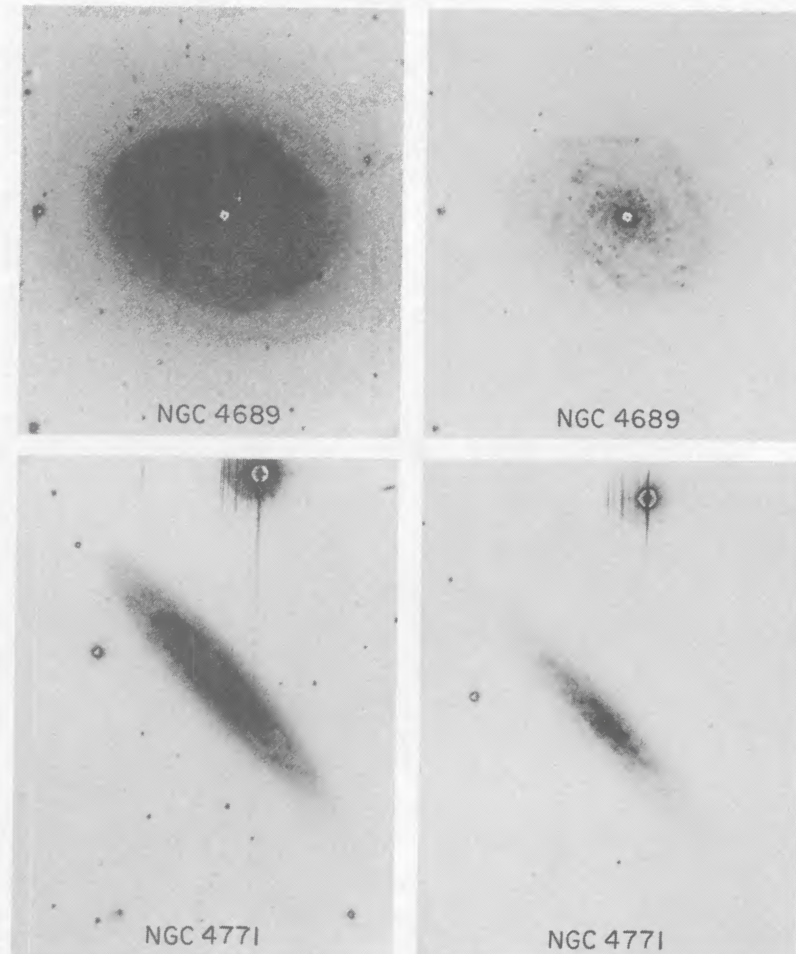

FIG. 2

FIG. 1.—Montage showing four examples of "Virgo-type" galaxies in which the saturated nuclear bulge contains a large number of bright young stars
FIG. 2.—High- and low-density images of two "Virgo-type" galaxies showing the concentration of star formation in the inner regions

old red stars. In such objects it is a bright central disk of luminous young (possibly reddened) stars that often mimics a central bulge on saturated photographic exposures. It is both interesting and significant that objects with this peculiar morphology are found to be exceedingly rare in the Ursa Major Cluster, which has a much lower density than the Virgo Cluster. Since the Virgo and Ursa Major clusters are at roughly the same distance, this difference cannot be ascribed to bias or selection effects. In the last column of Table 1 such "Virgo-type" galaxies are marked with an asterisk. Possibly the early-type spirals in the Virgo Cluster region, which exhibit star formation in their cores, represent a mild manifestation of the Butcher-Oemler (1978) effect that still persists at zero redshift.

IV. DISCUSSION

a) Frequency Distribution of Classification Types

Figure 3 shows a plot of DAO classification type versus apparent magnitude for galaxies in the Virgo Cluster proper and in the Ursa Major Cluster. The lack of objects in the lower part of these diagrams is due to both incompleteness *and* the fact that Hubble types become meaningless or ill-defined for spiral galaxies with $M_B \gtrsim -18$. The most striking difference between the Virgo and Ursa Major clusters is that early-type (E, S0, Sa) galaxies are much more frequent in the dense Virgo Cluster than they are in the more open Ursa Major Cluster. This phenomenon has been discussed previously by van den Bergh (1960*b*) and by Dressler (1980).

b) Tidal Effects

Tidal distortions, or the aftereffects of recent mergers, are most easily seen in spiral galaxies. Such effects were noted in three out of 37 spirals (8%) in the Ursa Major Cluster and in six out of 72 spirals (8%) in the Virgo Cluster proper. This may indicate that the higher space density of galaxies in Virgo is compensated for by the higher average speeds of encounter, which result in less severe tidal distortions. A possible caveat is, however, that a few galaxies which are strongly distorted by tidal interactions may have been omitted from the sample because of the possibility that they would deviate significantly from the mean Tully-Fisher relation.

If 8% of all spirals exhibit tidal distortions (or suffered recent mergers), and if such effects remain visible for $\sim 1 \times 10^9$ yr, then a typical spiral galaxy would be expected to suffer ~ 1 tidal encounter or merger with a gravitationally significant galaxy per Hubble time. This value may, in fact, be a lower limit to the actual number of tidal interactions suffered by a typical spiral, because the space density of galaxies in the early universe was considerably higher than it is at the present time.

c) Distance to the Virgo Cluster

Figure 4 shows a plot of B_T magnitudes versus luminosity classifications on both the DAO system (this paper) and on the RSA system (Sandage and Tammann 1981; Binggeli, Sandage, and Tammann 1985). Not plotted in this graph are galaxies with uncertain luminosity classifications, anemic galaxies, and objects that (on the basis of their position on the sky) were not regarded as members of the Virgo Cluster proper, or of the Ursa Major Cluster. Inspection of Figure 4 shows that the DAO classifications exhibit significantly less scatter than do those on the RSA system. This difference, which is largest for faint, low-surface brightness galaxies, is most likely due to the fact that the present digital data are superior to the photographic plates available to Sandage *et al.*

There is no *a priori* reason to believe that blue magnitudes of galaxies and their luminosity classifications are *linearly* correlated. A least-squares solution for the data plotted in Figure 4 therefore does not appear meaningful. To guide the eye a straight line, however, has been drawn through the DAO data in the left-hand panel of the figure. This line yields $\langle B_T \rangle =$ 10.85, 12.05, 12.7, and 13.3 for luminosity classes I–II, II–III, III, and III–IV, respectively. Adopting these values, together with the distances and absolute magnitudes (van den Bergh 1989) of the calibration galaxies in Table 2, yields a distance modulus $(m-M)_0 \simeq (m-M)_B = 31.12 \pm 0.38$ for members of the Virgo Cluster proper (the quoted error includes the uncertainty in the adopted calibration). The corresponding distance to the Virgo Cluster is $16.75^{+3.2}_{-2.7}$ Mpc. Note that this determination of the Virgo distance involves only (1) the distance determinations to the five fundamental calibrators (which are mainly based on observations of Cepheids and RR Lyrae stars) and (2) the assumption that there are no systematic differences

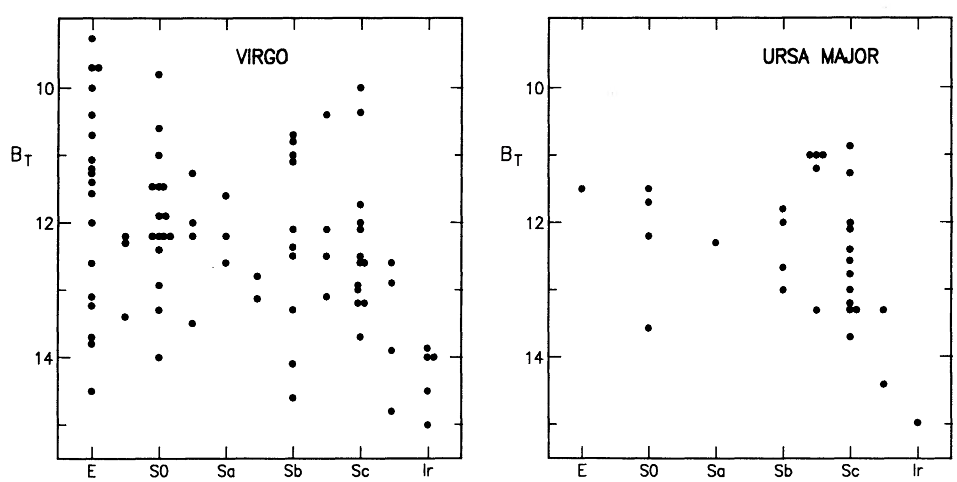

FIG. 3.—Magnitude vs. classification type for galaxies in the Virgo Cluster (*left*) and in the Ursa Major Cluster (*right*). Note the small relative frequency of early-type (E–Sa) galaxies in the low-density Ursa Major Cluster.

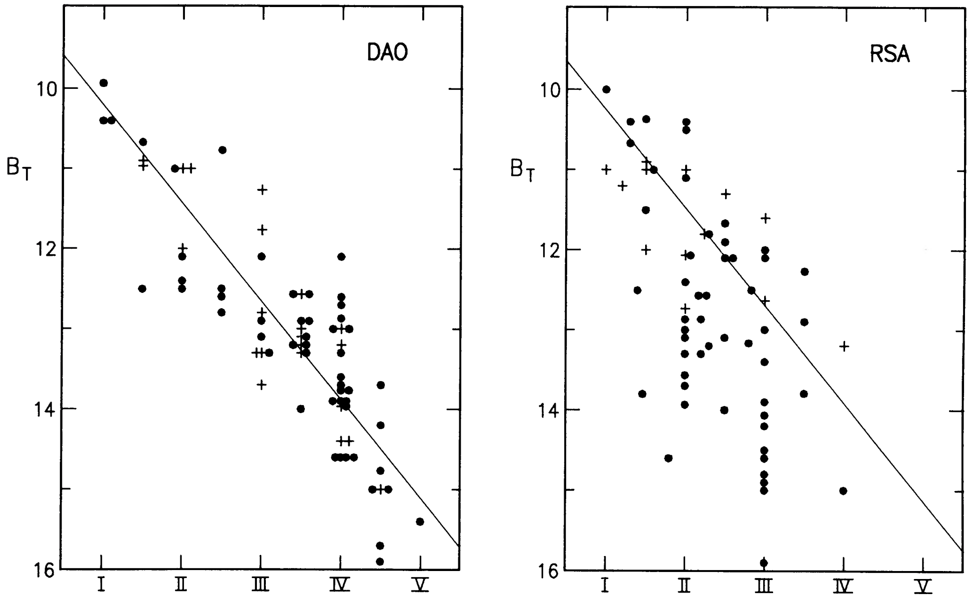

FIG. 4.—Luminosity class vs. apparent magnitude B_T for galaxies in the Virgo (*filled circles*) and Ursa Major (*plus signs*) clusters. New DAO classifications on left; RSA classifications on right.

between the luminosity classifications of these nearby standards and distant Virgo spirals.

The data in the left-hand panel of Figure 4 also show no significant difference in the distance moduli of the Virgo and Ursa Major clusters. The observed difference (in the sense Vir − UMa) is $\Delta(m-M)_B = +0.05 \pm 0.17$. In computing this difference, anemic galaxies, galaxies with uncertain luminosity classifications, and objects of luminosity classes IV–V and V (for which the data are very incomplete in luminosity) were omitted. For objects of luminosity classes I–IV the rms dispersion around the line drawn in the left-hand panel of Figure 4 is 0.68 mag. Since a few of the galaxies in the Virgo field are probably background (or foreground) objects, the intrinsic dispersion in the luminosity classification of galaxies with luminosity classes I–IV is $\lesssim 0.68$ mag, i.e., it is possible to estimate the luminosity of a spiral galaxy to slightly better than a factor of 2 from its morphology on a digital image. Luminosity classification techniques may therefore be used to test the assignment of some spirals to a cloud behind the Virgo Cluster by Tully and Pierce (1990).

d) Dispersion in Virgo Tully-Fisher Relation

The Tully-Fisher relation for the Virgo Cluster exhibits an unexpectedly large dispersion (Pierce and Tully 1988; van den Bergh 1989). This observation might be interpreted in one of two ways: either (1) the intrinsic dispersion in the Tully-Fisher relation increases dramatically in dense clusters such as Virgo, or (2) the Virgo Cluster sample is contaminated by background galaxies. Luminosity classification techniques make it possible to distinguish between these two alternatives. From the data given in Table 1, luminosity classifications (uncertain classifications and anemic galaxies excluded) for galaxies with luminosity classes in the range I–IV are available for 42 members of the Virgo Cluster proper. Of these, 37 have individual distances determined via the Tully-Fisher relation. From these TF distances eight galaxies are assigned to the background because they have $D > 20.0$ Mpc, and 29 are believed to be cluster members because they have $D < 20.0$ Mpc. Adopting the luminosity calibrations given in Table 3, the distance moduli for 29 members of the Virgo Cluster proper and for the eight background galaxies in the Virgo field are $\langle(m-M)_B\rangle = 30.93 \pm 0.13$ (15.3 Mpc) and $\langle(m-M)_B\rangle = 31.59 \pm 0.17$ (20.8 Mpc), respectively. The *difference* between the distance moduli of the TF background and cluster galaxies is therefore $\Delta(m-M) = 0.66 \pm 0.21$. The galaxy luminosity classifications therefore confirm the reality of cluster/background segregation based on the Tully-Fisher distance assignments at the $\sim 3\ \sigma$ level. In other words, *the luminosity classifications of individual galaxies strongly confirm the conclusion that inclusion of background galaxies in the Virgo sample contributes significantly to the observed dispersion in the Tully-Fisher relation for Virgo galaxies.*

The reality of the distance dispersion within the Virgo Cluster proper may also be tested by comparing distances

TABLE 2

DATA FOR CALIBRATION GALAXIES

Galaxy	DAO/DDO Type	$(m-M)_B$	B_T	M_B	$(m-M)_{\rm Virgo}$
LMC	Ir III–IV	18.75	1.00	−17.75	31.05
M31	Sb I–II	24.61	4.38	−20.23	31.08
M33	Sc II–III	24.95	6.26	−18.69	30.74
M81	Sb I–II	27.95	7.86	−20.09	30.94
NGC 2403	Sc III	27.96	8.89	−19.07	31.77

TABLE 3

ADOPTED CALIBRATION OF DAO LUMINOSITY CLASSES

Luminosity Class	B_T(Virgo)[a]	M_B
I	10.3	−20.8
I–II	10.85	−20.3
II	11.5	−19.6
II–III	12.05	−19.1
III	12.7	−18.4
III–IV	13.3	−17.8
IV	13.9	−17.2

[a] From left-hand panel of Fig. 3.

obtained from the Tully-Fisher relation and from luminosity classifications. Such a comparison shows a correlation coefficient $r = 0.44 \pm 0.14$ between distance moduli of members of the Virgo Cluster proper obtained from luminosity classifications and those obtained from the Tully-Fisher technique.

Excluding objects that, on the basis of the Tully-Fisher relation, are background objects, and adding a systematic mean error of 0.31 mag in quadrature to the 0.13 mag internal distance modulus error quoted above, yields $\langle (m-M)_B \rangle = 30.93 \pm 0.34$ ($15.3^{+2.6}_{-2.2}$ Mpc) for the core of the Virgo Cluster proper. This Virgo Cluster distance is, within its quoted errors, in excellent agreement with recent determinations using the Tully-Fisher technique (Pierce and Tully 1988) and planetary nebulae (Jacoby, Ciardullo, and Ford 1990).

e) *Velocity Dispersion*

Huchra (1985) finds that the velocity dispersion of galaxies in the Virgo Cluster is a function of Hubble type. The increased precision of such classifications that is possible on digital images makes it worthwhile to reinvestigate this dependence. Figure 5 shows a plot of the radial velocity V_0 as a function of Hubble type on the DAO system for members of the Virgo Cluster proper. The data plotted in this figure are consistent with Huchra's conclusion that Virgo ellipticals have a smaller velocity dispersion than do Virgo spirals, with S0 galaxies having intermediate characteristics. It should, however, be emphasized that a Kolmogorov-Smirnov test for the data plotted in Figure 5 shows that the kinematical differences between the E, S0, and spiral galaxies in the present sample are *not* statistically significant.

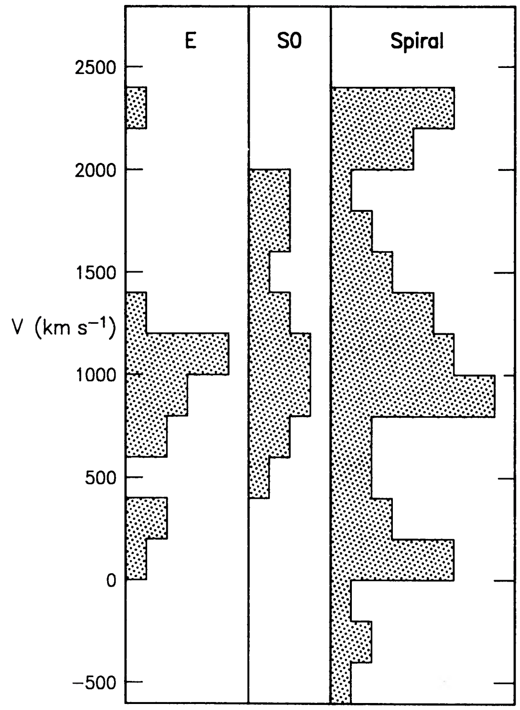

FIG. 5.—Radial velocity vs. Hubble type for galaxies in the Virgo Cluster proper. The figure suggests that ellipticals may have a smaller velocity dispersion than do spirals, with the velocity dispersion for S0 galaxies being intermediate between that for galaxies of types E and S. However, a Kolomogorov-Smirnov test shows that these differences are not statistically significant.

f) *Dust in Virgo and UMa Galaxies*

The spiral and irregular galaxies in the sample were divided into four classes on the basis of the amount of dust that was visible in their images: very dusty = 3, dusty = 2, little dust = 1, and no dust = 0. After excluding edge-on (and nearly edge-on) objects and anemic galaxies the "mean dustiness classes D" listed in Table 4 are obtained. These numbers, which are based on a sample of 68 objects, show that the mean dustiness of spiral and irregular galaxies in Virgo and Ursa Major drops precipitously below $B_T \simeq 13$ ($M_B \approx -18$). Since the stellar background density in digital galaxy images can be varied interactively at will, this effect is not (or at least not predominantly) due to the fact that it is easier to see dust on a bright stellar background than it is to detect it on a faint background. It seems highly likely that the low dust abundance in faint galaxies in and near the Virgo and Ursa Major clusters is a result of the well-known correlation between the luminosity and metal abundance of galaxies (cf. Skillman, Kennicutt, and Hodge 1989 and references therein). The low dust abundance in the LMC ($M_B = -17.8$), and the even lower dust abundance in the SMC ($M_B = -16.1$) (which have been reviewed by Israel 1984 and by Koornneef 1984), provide a nearby example of this phenomenon. This dependence of dustiness of late-type galaxies on their luminosity will be discussed in more detail in van den Bergh and Pierce (1990).

g) "*Virgo-Type*" *Galaxies*

The Virgo Cluster region contains a large number of peculiar objects with fuzzy outer regions, which exhibit active star formation in their central bulges (disks?). Objects of this type, which we refer to as "Virgo-type" galaxies, are illustrated in Figures 1 and 2. Of the spiral galaxies in the Virgo Cluster proper, 27 out of 62 (44%) are of the Virgo type. Among spiral galaxies in the Vir SE, Vir E, and Vir W subclusterings, 11 out of 26 (42%) are also of the Virgo type. Since there appears to be no difference between the Virgo Cluster proper and these sub-

TABLE 4

$\langle D \rangle$ VERSUS B_T FOR UMA AND VIRGO GALAXIES

Galaxy Magnitude	$\langle D \rangle$
$10.0 \le B_T < 11.0$.....	1.8
$11.0 \le B_T < 12.0$.....	1.6
$12.0 \le B_T < 13.0$.....	1.5
$13.0 \le B_T < 14.0$.....	0.7
$14.0 \le B_T < 15.0$.....	0.3

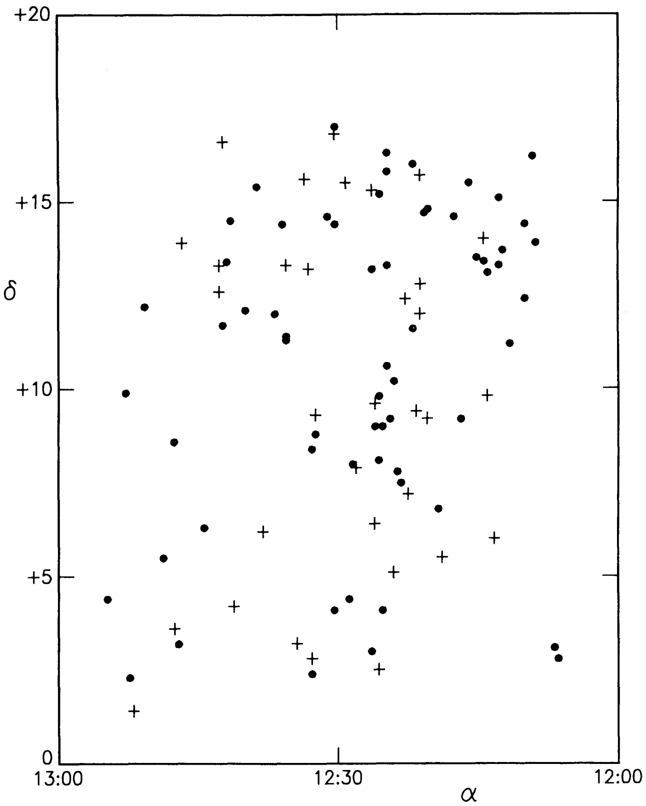

FIG. 6.—Positions of normal spirals (*filled circles*) and of Virgo-type objects (*plus signs*) in the Virgo region. No obvious differences are seen between the distributions of these two types of objects on the sky.

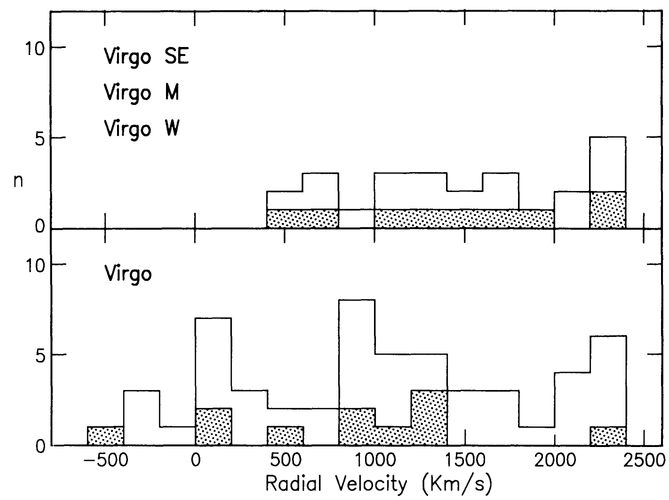

FIG. 7.—Comparison of the radial velocities of spiral galaxies in the Virgo Cluster proper with those of spirals in the Vir SE, Vir M, and Vir W regions. "Virgo-type" spirals are shown by heavy shading. The figure shows no significant difference between normal spirals and "Virgo-type" objects. Note, however, that on average Vir SE, Vir M, and Vir W galaxies have larger radial velocities than do spirals in the Virgo Cluster proper.

regions, we shall combine the data for the entire Virgo region, yielding 38 out of 88 (43%) of all spirals of Virgo type. This contrasts with the situation in the Ursa Major Cluster, in which only two out of 35 spirals (6%) were found to be of the Virgo type. Another difference between the galaxy populations of these two areas is that very open late-type spirals occur in UMa (and in other field areas) but *not* in the Virgo region. It is still too early to say whether all Virgo-type objects arrived at their present morphological state via similar evolutionary paths.

Figure 6 shows no obvious difference between the spatial distribution of Virgo-type objects and that of normal spirals in the Virgo region. By the same token, Figure 7 shows no significant differences between the radial velocity distributions of Virgo type galaxies and that of Virgo spirals. This figure does, however, illustrate the well-known fact that objects in the Vir SE, Vir M, and Vir W regions exhibit a larger average redshift than do those in the Virgo Cluster proper.

V. CONCLUSIONS

Morphological classifications of 231 galaxies in and near the Virgo and Ursa Major clusters show that luminosity classification techniques can be used to determine the luminosities of spiral galaxies with an accuracy of ~0.7 mag on CCD frames. In the direction of the Virgo Cluster the present observations confirm the assignment of some galaxies to the background field. This observation strongly confirms the conclusion that the large dispersion in the Tully-Fisher relation for Virgo galaxies is, at least in part, due to contamination of the Virgo core sample by background galaxies.

Using the LMC, M31, M33, M81, and NGC 2403 as calibrators, luminosity classification techniques yield a distance of $15.3^{+2.6}_{-2.2}$ Mpc for the spiral and irregular galaxies associated with the core of the Virgo Cluster proper. Furthermore, the Ursa Major and Virgo cluster distances are found to be the same, within the accuracy that is provided by luminosity classification techniques.

A class of galaxies with fuzzy anemic outer structure and active star formation in their cores is found to be common in Virgo, but rare in the Ursa Major Cluster. Finally, the dustiness of galaxies in and near these two clusters is found to drop dramatically below $B_T \simeq 13$ ($M_B \simeq -18$). This effect is most plausibly attributed to a dependence of the heavy-element abundance in the interstellar gas on the luminosity of spiral and irregular galaxies.

REFERENCES

Binggeli, B., Sandage, A., and Tammann, G. A. 1985, *A.J.*, **90**, 1681.
Butcher, H., and Oemler, A. 1978, *Ap. J.*, **219**, 18.
de Vaucouleurs, G. 1961, *Ap. J. Suppl.*, **6**, 213.
Doyon, R., and Joseph, R. D. 1989, *M.N.R.A.S.*, **239**, 347.
Dressler, A. 1980, *Ap. J.*, **236**, 351.
Giovanelli, R., and Haynes, M. P. 1985, *Ap. J.*, **292**, 404.
Gunn, J. E., and Gott, J. R. 1972, *Ap. J.*, **176**, 1.
Haynes, M. P., and Giovanelli, R. 1986, *Ap. J.*, **306**, 466.
Huchra, J. P. 1985, in *The Virgo Cluster*, ed. O.-G. Richter and B. Binggeli (Garching: ESO), p. 181.
Huchra, J. P., Davis, M., Latham, D., and Tonry, J. 1983, *Ap. J. Suppl.*, **52**, 89.
Israel, F. P. 1984, in *IAU Symposium 108, Structure and Evolution of the Magellanic Clouds*, ed. S. van den Bergh and K. S. de Boer (Dordrecht: Reidel), p. 319.
Jacoby, G. H., Ciardullo, R., and Ford, H. C. 1990, *Ap. J.*, **356**, 332.
Kenney, J. D. P., and Young, J. S. 1989, *Ap. J.*, **344**, 171.
Koornneef, J. 1984, in *IAU Symposium 108, Structure and Evolution of the Magellanic Clouds*, ed. S. van den Bergh and K. S. de Boer (Dordrecht: Reidel), p. 333.
Pierce, M. J. 1988, Ph.D. thesis, University of Hawaii.

Pierce, M. J., and Tully, R. B. 1988, *Ap. J.*, **330**, 579.
Sandage, A., and Tammann, G. A. 1981, *A Revised Shapley-Ames Catalog of Bright Galaxies* (Washington, DC: Carnegie Institution of Washington).
Skillman, E. D., Kennicutt, R. C., and Hodge, P. 1989, *Ap. J.*, **347**, 875.
Tully, R. B. 1988, *Nearby Galaxies Catalog* (Cambridge: Cambridge University Press.
Tully, R. B., and Pierce, M. J. 1990, in preparation.
van den Bergh, S. 1960*a*, *Ap. J.*, **131**, 215.
———. 1960*b*, *Ap. J.*, **131**, 558.
———. 1960*c*, *Pub. David Dunlap Obs.*, **2**, 159.
———. 1966, *A.J.*, **71**, 922.
van den Bergh, S. 1976*a*, *Ap. J.*, **206**, 883.
———. 1976*b*, in *The Galaxy and the Local Group*, ed. R. J. Dickens and J. E. Perry (*RGO Bull.*, No. 182; Herstmonceux: Royal Greenwich Observatory), p. 98.
———. 1984, *A.J.*, **89**, 608.
———. 1989, *Astr. Ap. Rev.*, **1**, 111.
van den Bergh, S., and Pierce, M. J. 1990, in preparation.
van Gorkom, J., and Kotanyi, C. 1985, in *The Virgo Cluster* ed. O.-G. Richter and B. Binggeli (Garching: ESO), p. 61.
Zasov, A. V. 1975, *Soviet Astr.—AJ*, **18**, 426.

Note added in proof.—Recently L. Vigroux, O. Boulade, and J. A. Rose (*A.J.*, **98**, 2044 [1989]) have also found evidence for a low-level kind of Butcher-Oemler effect in clusters at low redshift.

Michael J. Pierce and Sidney van den Bergh: Dominion Astrophysical Observatory, 5071 W. Saanich Road, Victoria, BC Canada, V8X 4M6

R. Brent Tully: Institute for Astronomy, 2680 Woodlawn Drive, Honolulu, HI 96822